A FINITE ELEMENT COMPARISON BETWEEN TWO SIZES OF NiTi COMMERCIAL STAPLES USED IN SCAPHOID FRACTURE FIXATION

M. Kh. MAJD [1], *M. BAHRAMI* [2], *A. NOURI* [1], *M. H. NAZARPAK* [3]

[1] *Department of Biomedical Engineering, Amirkabir University of Technology (Tehran Polytechnic), Tehran, Iran;*

[2] *Department of Mechanical Engineering, Faculty of Engineering, University of Kashan, Kashan, Iran;*

[3] *New Technologies Research Center, Amirkabir University of Technology (Tehran Polytechnic), Tehran, Iran*

Most carpal bone fractures occur in the scaphoid. This work is aimed at finding the most suitable size of NiTi shape memory alloy (nitinol) staples to heal scaphoid fractures by comparing two commercially available compression staples (DynaClip™ Bone Fixation System, 10×10 and 14×14 mm). In the present study the scaphoid bone was selected for simulating a model in SolidWorks software. To accurately investigate the effect of staple size on the bone the scaphoid was assumed to be a three-layer composite structure consisting of collagen and mineral crystals. The stress distributions along a path located at the waist of the scaphoid were assessed. The finite element analysis was carried out in ABAQUS software based on the nitinol staple shape memory effect and super-elasticity behavior. The results indicated that the smaller size of staples induced a more significant stress on the central zone of the scaphoid, whereas the larger size of staples showed a peak stress concentration on the peripheral zones with a reduced stress concentration at the center. Hence, it is suggested to utilize the two of these staples in different orientations or in parallel with each other to improve the biomechanical behavior of the regenerated bone.

Keywords: *bone fracture, bone healing, shape memory NiTi alloy, staple, finite element, scaphoid, simulation.*

Оскільки переломи зап'ястних кісток найчастіше відбуваються в човноподібній кістці, здійснено пошук найвідповіднішого розміру скоб зі сплаву NiTi (нітинолу) з ефектом пам'яті форми для їх зрощення. Порівняно дві компресійні скоби (DynaClip™ Bone Fixation System, 10×10 і 14×14 mm). З допомогою програми SolidWorks створено модель, щоб детально вивчити вплив розміру скоб на кістку. Вважали, що човноподібна кістка є тришаровою композитною структурою, яка складається з колагену та мінеральних кристалів. Оцінено розподіл напружень уздовж вигнутої її середини. Метод скінченних елементів реалізувано за допомогою програмного забезпечення ABAQUS на основі нітинолових скоб з ефектом пам'яті форми і надпружних режимів. Встановлено, що за меншого розміру скоб відчутніше діють напруження на центральну зону кістки, тоді як за більшого – концентруються на периферійних зонах. Тому запропоновано використовувати ці скоби в різних орієнтаціях або паралельно одна до одної, щоб поліпшити біомеханічну поведінку регенерованої кістки.

Ключові слова: *перелом кістки, зрощення кістки, сплав з ефектом пам'яті форми NiTi, скоба, скінченний елемент, човноподібна кістка, моделювання.*

Introduction. Shape memory alloys (SMAs) have been used in recent decades in different applications such as automotive, aerospace, and medicine [1]. The most popular SMA is nickel-titanium alloy (NiTi alloy, also known as nitinol) [2]. Two distinctive properties of nitinol are shape memory effect and super-elasticity. The capability of these materials to recover their initial shape after being subjected to large strains lies in

Corresponding author: M. Kh. MAJD, e-mail: yscmsse2021@gmail.com

the aforementioned properties, making them a popular biomaterial [3]. SMAs have two phases called martensite (cold phase) and austenite (hot phase). The shape memory effect and super-elasticity of the SMA materials lead to the recovery of their initial shape after large strains, which emerge as a result of these two-phase shifts in which the crystal structures are rearranged [3, 4].

In addition, the biocompatibility of nitinol has made it an attractive material in biomedical fields. This material found applications in vascular and nonvascular stents, orthopedic fixations, orthodontic wires, and ear implants [5, 6]. One of the most famous NiTi devices in orthopedic applications is the staple, which is a common method of fixing fractures in small bones. Some examples of using nitinol staples are scaphoid fractures, inter-carpal fusion, patellar fractures, ligament fixation, facial fractures, and spinal procedures [7]. One of the advantages of using bone staples instead of other fixation methods is that they reduce the time and difficulty of surgery, cause no stress shielding, unlike other fracture fixation devices, and lead to minimal bone tissue damage caused by perforation. The staple applies a compression force across the fractured segment, increasing the pace of bone fracture healing by preventing an excessive amount of movement in the healing process [8, 9]. Nitinol staples produce the adequate compression needed for the assimilation of the fracture sites [9]. Since the scaphoid is the most frequently fractured carpal bone, scaphoid fractures are the point of focus in the present study.

It is still unclear how staple size affects the biomechanics of fractured bones as well as the speed and quality of healing. Investigations on bone staples have been primarily conducted in laboratories. The main issues with laboratory experiments are their costs and the differences in conditions that may occur in each experiment. The factors like bone or bone substitute properties, staple material components, fabrication defects, and mechanical behaviors of bone and staple are not exactly alike in every experimental test. Their footprints can be seen in the results of the tests, making them less accurate. The mentioned problems could be minimized by designing and simulating the exact bone and staple in SolidWorks and ABAQUS software. In the past, the mechanical behavior of a model was defined and known through repetitive experiments and prototyping. To decrease the time and increase the accuracy of the tests, finite element analysis (FEA) has been developed [3]. Fortunately, current commercially available software can be considered suitable platforms for simulating and analyzing SMA-made models. ABAQUS is famous FEA software that can analyze the stress and displacement produced by the staple and distributed in the scaphoid waist as the staple tries to regain its initial shape. SolidWorks software was used to design the form of the staple and scaphoid anatomy.

Moreover, using a computer simulation, it is easier and more cost-effective to optimize the size of the staples based on their biomechanical behavior and mechanical properties. The staple size can affect the stress contour in the position of the fracture. Stress can affect the process of bone healing [10–18]. Moreover, the bone configuration and mechanical properties are other factors that determine the stress concentration areas and stress contour on the fracture surface. In the present study, the specific configuration and properties of the scaphoid were simulated to investigate the biomechanics of nitinol bone staples on cubic bone simulations [1, 9]. The objective of this study is to compare the stress distribution patterns of two different sizes of nitinol staples to find the best staple size for scaphoid fracture fixation.

Modeling and simulation. To mimic natural scaphoid fracture fixation, a complete modeling of the scaphoid bone and two staples (DynaClip™ Bone Fixation System, 10×10 and 14×14 mm) in different sizes, suitable for scaphoid fractures, was performed based on DynaClip catalog data [19].

For modeling the scaphoid, a human scaphoid bone (from the Iran University of Medical Science) was used, and 16 pictures were captured from the bone every 22.5° (Fig. 1). These pictures were then utilized to model the exact shape of the scaphoid in

SolidWorks. The size of the scaphoid, moreover, was taken from an experiment finding the mean size of the scaphoid from 14 cadaver scaphoid bones [3].

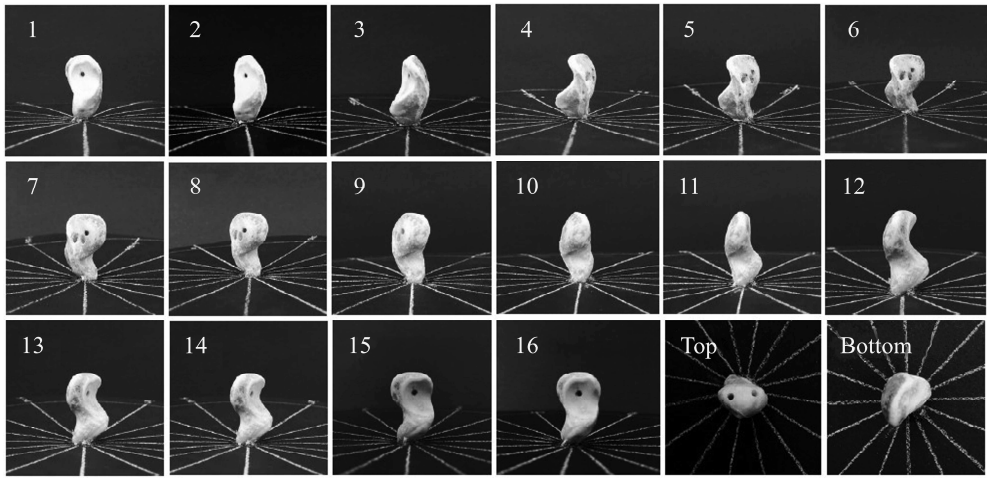

Fig. 1. Scaphoid bone images, captured from the real bone at every 22.5°.

Bone simulation. For modeling the scaphoid material, bone was considered a two-phase composite in which the mineral and collagen were bound in a complex manner [20]. At the nano-structural level, the bone can be considered a platelet-reinforced composite material consisting of hydroxyapatite mineral crystals (reinforcement phase) distributed within organic collagen fibrils (compliant matrix phase), whose properties are reported in Table 1 [21]. The scaphoid is the most frequently fractured carpal bone, often occurring after a fall onto an outstretched hand. As some epidemiological information indicates, 15% of acute wrist injuries and 60% of all carpal fractures are dedicated to the scaphoid bone. Most scaphoid fractures occur at the waist (65...68%) and 37% of total fractures are in transversal orientation at the waist of the scaphoid. To specify the mandatory research on the scaphoid, it can be mentioned that the major and minor blood supplies enter the scaphoid from different locations and supply 80% and 20% of the scaphoid via retrograde blood flow, respectively. These blood supplies consequently create a poor fracture healing environment in the bone [22]. After a scaphoid fracture, disruption in these supplies causes a significant rate of nonunion. Nonunion may disrupt blood flow and cause additional problems, such as inflammation and pain for the patient [22, 23]. Accordingly, the scaphoid 3D averaged bone density model displayed a specific volumetric bone mineral density (vBMD) distribution pattern. Three zones are identified, demonstrating high, intermediate, and low vBMD values. High-density values are located in the peripheral zone of the scaphoid, corresponding to areas with the dense cortical and subchondral zone. The intermediate zone, with four different sub-regions, has been categorized inside this peripheral zone. The properties of these parts of the bone are summarized in Table 2. It can be seen that the lowest vBMD values are observed at the center of the scaphoid [24].

Table 1. Mechanical properties of composite phases

Material	Young's modulus *E*, GPa	Poisson ratio
Hydroxyapatite	114	0.28
Collagen	1.2	0.35

Table 2. Mechanical properties of the scaphoid six zones (including sub-regions)

Bone zone	V_{total}, mm^3	mgHA / cm^3	HA, g	HA, vol.%	$E_{comp.}$, GPa	$v_{comp.}$
Peripheral zone	726.83	549.4	0.399	17.37	20.79	0.33
Medial subregion	315.01	376.2	0.118	11.85	14.56	0.34
Subregion near the proximal pole	460.73	379.0	0.174	11.85	14.67	0.34
Subregion near the distal pole	437.48	346.5	0.151	10.92	13.51	0.34
Lateral subregion	248.05	389.1	0.096	12.24	15.0	0.34
Center zone	1280.19	225.6	0.268	7.11	9.22	0.34
Total	3468.29	–	1.226	71.44	–	–

The modeling procedure in which the scaphoid is designed in SolidWorks was then improved in ABAQUS by modeling the three-part structure of the scaphoid and assigning different mechanical properties to them. The data on their mechanical properties were calculated by the mixture law from their mineral and collagen matrix percentages. Moreover, the volume of these parts was determined separately and proportional to the simulated model (see Table 3).

Table 3. Mechanical properties of the three zone of the bone simulated ABAQUS

Bone zone	V_{total}, mm^3	Young's modulus E, GPa	Poisson ratio
Center	1280.19	9.22	0.34
Intermediate	1461.27	14.35	0.34
Peripheral	726.83	20.79	0.33

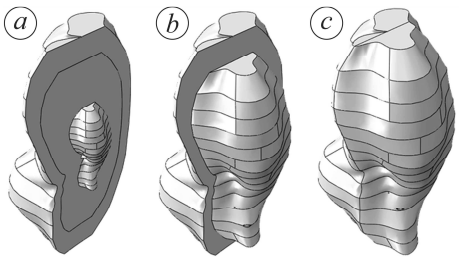

Fig. 2. Center (*a*), intermediate (*b*) and peripheral (*c*) zones of scaphoid.

Since the mechanical properties of the bone highly depend on its mineral composition, the scaphoid model was defined in three parts (Fig. 2), each with different mechanical properties. A bone like scaphoid consists of three types of bones with different mechanical properties, thus the stress made from NiTi staples can vary in different parts of the bone and cause a non-unified stress distribution alongside the fracture surface. This phenomenon can affect the regenerated bone mineralization and change the initial structure of the bone, causing the creation of possible fracture areas. Moreover, in order to evaluate the potential damage to the bone, plastic deformation data for the average trabecular bone, which has the most similar mechanical properties to the middle part of the scaphoid, was used.

Staple simulation. For simulating the staple, the first step was designing its shape. The models were derived from the commercially available nitinol staples (DynaClip™ Bone Fixation System), usually used in fracture fixation of the scaphoid. In the guide catalog of these staples, the suitable staple size for this fixation was determined as 10×10 mm, 12×12 mm, and 14×14 mm, so in this research, the 10×10 mm and 14×14 mm

staples were subjected to comparison (Fig. 3). The dimensions of the staple were given in the brochure data (MedShape, Inc., 2019) [19].

The next step of the simulation was defining the NiTi shape memory alloy material for the designed staple in ABAQUS. The data required for this definition were collected at an A_f of 37°C and are shown in Table 4 and Fig. 4.

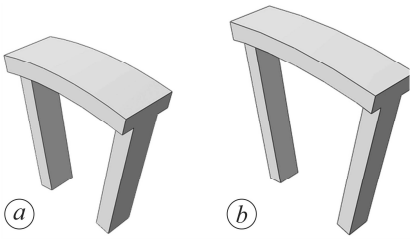

Fig. 3.

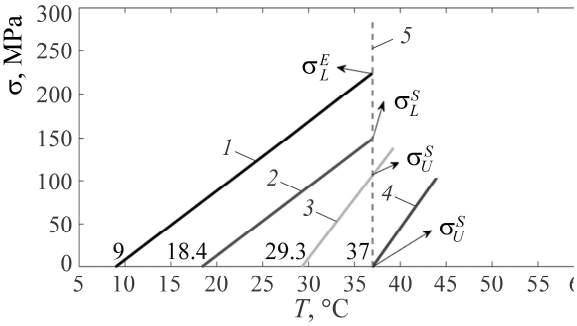

Fig. 4.

Fig. 3. 10×10 mm nitinol staple (*a*), 14×14 mm (*b*) nitinol staple.

Fig. 4. Stress vs. temperature curve of nitinol: *1* – martensite end; *2* – martensite start; *3* – austenite start; *4* – austenite end; *5* – T_0 = 37°C.

Table 4. Mechanical properties of nitinol [25]

Mechanical properties	Value
E_a, MPa	26300
E_m, MPa	63000
M_f, °C	9
M_s, °C	18.4
A_s, °C	29.3
A_f, °C	37
C_M, MPa/°C	8
C_A, MPa/°C	13.8
σ_s^{cr}, MPa	100
σ_f^{cr}, MPa	170
ε^*	0.067

The meshing type of the bone was tetrahedral (linear for the whole model except ± 0.3 mm belt in the fracture site, the waist of the scaphoid where the fractures are most likely to occur, and it is the case of study in this research, which was quadric). The meshing type for staple was linear tetrahedral.

The procedure was simulated in two steps. In the first step, the staple legs were subjected to uniform pressure, causing them to have enough displacement to enter the bone. In the second step, the force was deactivated, and the contact between bone and

staple legs was defined. Simultaneously, the temperature rose from 21 to 38°C, causing the total phase transformation in the staple from martensite to austenite and gradually regaining its initial shape. In an attempt to restore the original shape, the staple is pushed inside the bone and compresses both sides of the scaphoid bone. This pressure was illustrated in the path located at the waist of the scaphoid, parallel to the staple legs. To simplify the computations, the drill holes were modeled with rectangular cross-sections instead of circular ones. The effect of this can be negligible since the position of evaluation is in the waist of the bone, having a significant distance from the drill holes. Moreover, the surface of the staple and bone was considered smooth.

Results and discussion. All simulations were conducted with the "Static General" solver in ABAQUS. The results are time-independent, and the variants are temperature and pressure applied to the staple legs. These simplifications are the same in both analyses. Simulation processes and steps were defined as the clinical process of setting NiTi bone staples in the fractured scaphoid. After inserting the deformed staple in the drill holes of the bone and increasing the temperature (≥ 37°C), the staple starts to return to its original shape and, by doing so, produces compression forces alongside the bone. The scaphoid has a unique shape with a concave area on its waist, making compression pressure distribution different on its waist. There are two reasons why it is important to have a unified stress distribution on the fracture surface. The first is that contact healing is desired for fracture healing. Healing procedures are divided into two major groups: direct (primary) and indirect healing (secondary). Indirect fracture healing is the most common form of fracture healing, consisting of both endochondral and intramembranous bone healing. By contrast, direct (the aim of the current study) healing does not commonly occur in the natural process of fracture healing, and it is the goal of applying fixations to the fracture site [26]. Primary healing is the kind of healing that happens in the NiTi staple bone fixation method [7]. The other reason is that unified pressure distribution creates a similar healing environment for the fracture surface. Some studies have shown that compression force can alter the mechanical properties and mineral density of the regenerated bone [27]. Moreover, a study demonstrated that compression force significantly altered bone morphogenic protein 2 (BMP-2) secretion in large bone defect repair by increasing bone formation and modulating tissue organization and differentiation [28, 11].

In the first simulation, the investigations were carried out on the smaller staple (DynaClip™ Bone Fixation System, 10×10 mm). The visualization of the simulation is shown in Fig. 5*a* and the Von Mises stress produced by the staple versus distance from the staple bridge alongside its legs is illustrated in Fig. 6*a*. The maximum amount of stress is in the center of the bone, where there is the least amount of mineral composition. This amount decreases as the evaluation reaches peripheral zones.

It can be seen from Fig. 6 that there are four discontinuities between the first and last points of the path. The reason for which they happen is the border between two zones of the bone with different materials. Indeed, ABAQUS has identified one node related to two elements in non-identical zones. Each zone has its own specified Young's modulus, whereas both of them have the same strain. As a result of these statements and according to Hooke's law, two different stresses were calculated and reported for the node.

In the second simulation, the investigations were performed on the larger staple (DynaClip™ Bone Fixation System 14×14 mm, Fig. 5*b*). Since the staple legs are longer in this staple, the area of the bone on which the staple makes contact in the first place is further from the staple bridge, causing the maximum amount of stress on the peripheral zone. It is shown in Fig. 6*b* that the stress distribution decreases on the parts near the staple bridge. Although the maximum stress of 14×14 mm staple is lower

compared to the smaller staple, the area subjected to the compression stress is larger in the second investigation.

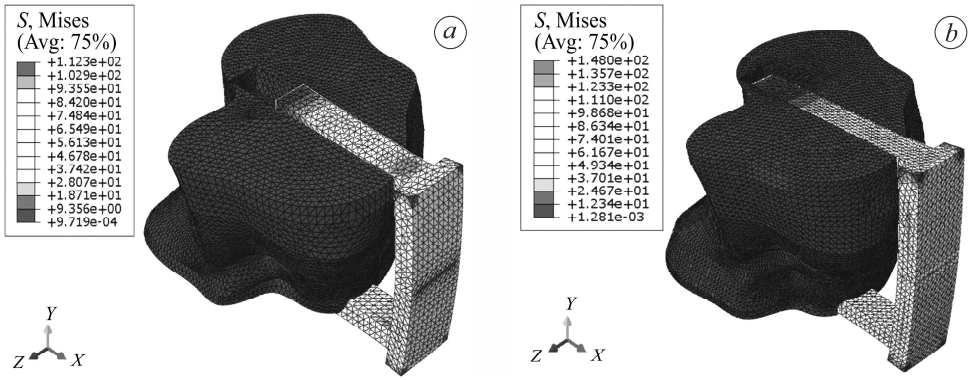

Fig. 5. Visualization of 10×10 mm (*a*) and 14×14 mm (*b*) staple (stress line is in MPa).

The maximum stress in the larger staple occurs in the furthest peripheral zone from the staple bridge, and it decreases as the evaluation becomes closer to the staple bridge in a linear path. This stress fades in the areas near the staple bridge (Fig. 6*b*). It can be anticipated that the bone regeneration algorithm would not be uniform along the fracture surface. As mentioned, stress can affect the mechanical properties of regenerated bone. The magnitude of stress and strain can also determine the type of healing: intramembranous and endochondral ossification [10, 11, 18]. Some studies demonstrated that constant high magnitudes of stress can have a negative impact on bone healing [27, 29]. On the other hand, some claimed that loading could elevate the secretion of chemical signaling factors for osteogenesis [17]. This information demonstrates the value of researching fixation techniques and the mechanical conditions they produce for fractured bones.

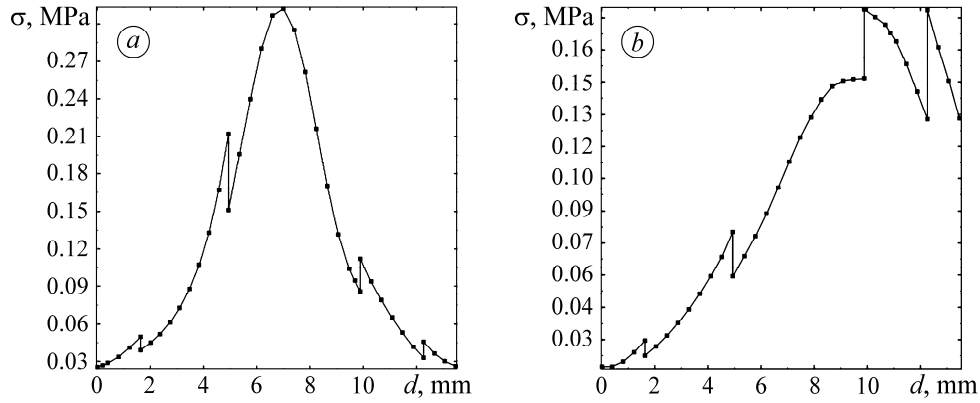

Fig. 6. Stress vs distance from staple bridge curve for 10×10 mm (*a*) and 14×14 mm (*b*) staple alongside a similar path.

Studies have also shown that some of the Ti fixations can provide the fracture site with a degree of motion, which accelerates the healing process [18]. The NiTi alloy used in this study has less rigidity than Ti, making it a more suitable material for the fabrication of fracture fixation devices.

A study on mouse tibia osteotomies healing under different external loadings demonstrated the effect of load on regenerated bone properties. It was reported that a moderate external loading could increase the callus strength, while higher loadings had adverse effects. It was also mentioned that a proper delay for applying fixations is well

desired to improve the mechanical strength of the regenerated bone. The proper amount of external load and delay for human scaphoid fracture healing have not yet been estimated, and thus further investigation is needed in this area [27]. The values of compression stress obtained here are of the same order as data reported in the literature for an in vitro study of SMA staples for internal fixation [30]. To simplify the software analyses and shorten the runtime, two parts of the bone where the study was performed were ignored. The reason for which this assumption was made is that the article approach is to evaluate the biomechanical behavior of the bone under stress produced by the staple. Hence, the parts that are above the staple leg do not have a significant effect on the obtained values. Therefore, the analyses were done on the parts of the bone between the staples leg and the other parts were omitted.

CONCLUSION

In the present study, a computational comparison was made between two NiTi staples of different sizes, suitable for scaphoid fracture fixation. The scaphoid bone, NiTi staples, and the applied stress at the fracture sites were simulated and analyzed using SolidWorks and ABAQUS software. The smaller staple caused higher stress concentration in the center and little or no stress concentration in the peripheral zones. On the other hand, the larger staple exhibited a peak stress concentration in the peripheral zones in the furthest areas from the staple bridge, with a reduced stress concentration at the center. Based on the simulation results, uniform stress distribution did not appear in any of the staples, and therefore it can be anticipated that proper bone regeneration is unlikely to occur. Further investigations are needed to design staples that produce uniform stress along the fracture surface.

1. *Saleeb A., Padula S. and Kumar A.* A multi-axial, multimechanism based constitutive model for the comprehensive representation of the evolutionary response of SMAs under general thermomechanical loading conditions // Int. J. of Plasticity. – 2011. – **27**, № 5. – P. 655–687.
2. *Klaput J.* Studies of selected mechanical properties of NiTinol shape memory alloy // Archiv. of Foundry Eng. – 2010. – **10**. – P. 155–158.
3. *Hatira F. B. and Saidane K.* A Thermo-mechanical behavior simulation of a NiTi staple used for the correction of idiopathic scoliosis // J. of Biomat. and Nanobiotechn. – 2012. – **3**, № 1. – P. 61–69.
4. *Concilio A. and Lecce L.* Shape Memory Alloy Engineering: For Aerospace, Structural and Biomedical Applications (1st ed.). – Butterworth-Heinemann, 2014. – 887 p.
5. *Analysis* of the whole implementation process and optimization of a Nitinol superelastic stent / X. M. Wang, P. Liu, H. Liang, M. C. Zhang, L. Li, and Z. F. Yue // Materialwissenschaft und Werkstofftechnik. – 2019. – **50**, № 1. – P. 44–51.
6. *Numerical* simulation of the force generated by a superelastic NiTi orthodontic arch wire during tooth alignment phase: comparison between different constitutive models / M. Gannoun, M. L. Hellara, C. Bouby, T. Ben Zineb, and T. Bouraoui T. // Mat. Res. Express. – 2018. – **5**, № 4. – Article number: 045405.
7. *Fracture* fixation using shape-memory (ninitol) staples / J. C. Wu, A. Mills, K. D. Grant, and P. J. Wiater // Orthopedic Clinics of North America. – 2019. – **50**, № 3. – P. 367–374.
8. *Russell S. M.* Design considerations for nitinol bone staples // J. of Mat. Eng. and Performance. – 2009. – **18**, № 5–6. – P. 831–835.
9. *Salameh T. M.* Performance of existing bone staples for treatment of fractures // Master thesis. – Clevland State University, 2020.
10. *Claes L. and Heigele C.* Magnitudes of local stress and strain along bony surfaces predict the course and type of fracture healing // J. of Biomechanics. – 1999. – **32**, № 3. – P. 255–266.
11. *Görlitz S.* The role of mechanical forces in osteogenic differentiation, BMP signaling and early tissue formation processes in the context of bone healing // PhD thesis. – Technische Universitaet Berlin, 2021.
12. *In vivo* loading increases mechanical properties of scaffold by affecting bone formation and bone resorption rates / A. Roshan-Ghias, F. M. Lambers, M. Gholam-Rezaee, R. Müller, and D. P. Pioletti. – Bone, 2011. – **49**, № 6. – P. 1357–1364.

13. *Effects* of in vivo mechanical loading on large bone defect regeneration / J. D. Boerckel, Y. M. Kolambkar, H. Y. Stevens, A. S. Lin, K. M. Dupont, and R. E. Guldberg // J. of Orthopaedic Res. – 2011. – **30**, № 7. – P. 1067–1075.
14. *Loading* induces site-specific increases in mineral content assessed by microcomputed tomography of the mouse tibia / J. Fritton, E. Myers, T. Wright, and M. Vandermeulen. – Bone, 2005. – **36**, № 6. – P. 1030–1038.
15. *3D strain* map of axially loaded mouse tibia: a numerical analysis validated by experimental measurements / V. A. Stadelmann, J. Hocké, J. Verhelle, V. Forster, F. Merlini, A. Terrier, and D. P. Pioletti // Computer Methods in Biomechanics and Biomedical Eng. – 2009. – **12**, № 1. – P. 95–100.
16. *Non-invasive* axial loading of mouse tibiae increases cortical bone formation and modifies trabecular organization: A new model to study cortical and cancellous compartments in a single loaded element / R. L. De Souza, M. Matsuura, F. Eckstein, S. C. Rawlinson, L. E. Lanyon, and A. A. Pitsillides. – Bone, 2005. – **37**, № 6. – P. 810–818.
17. *Nomura S. and Takano-Yamamoto T.* Molecular events caused by mechanical stress in bone // Matrix Biology. – 2000. – **19**, № 2. – P. 91–96.
18. *The investigation* of bone fracture healing under intramembranous and endochondral ossification / S. Ghimire, S. Miramini, G. Edwards, R. Rotne, J. Xu, P. Ebeling, and L. Zhang // Bone reports. – 2020. – **14**. – Article number: 100740.
19. *DYNACLIP* – Djo Global. https://www.djoglobal.com/sites/default/files/DynaClip%20 Procedure%20Guide_Rebranded.pdf.
20. *A three-dimensional* laminated paper model of the scaphoid from computed tomography / H. Kakizawa, N. Toyota, Y. Akiyama, Y. Kijima, O. Ishida, and K. Ito // Acta Radiol. – 2007. – **48**, № 1. – P. 80–88.
21. *Rho J. Y., Kuhn-Spearing L., and Zioupos P.* Mechanical properties and the hierarchical structure of bone // Medical Eng. and Phys. – 1998. – **20**, № 2. – P. 92–102.
22. *Vaughan T., McCarthy C., and McNamara L.* A three-scale finite element investigation into the effects of tissue mineralization and lamellar organization in human cortical and trabecular bone // J. of the Mech. Behavior of Biomedical Mat. – 2012. – **12**. – P. 50–62.
23. Scaphoid Fracture – Hand – Orthobullets /M. J. Steffes, J. H. Wang, D. D. Adams, J. Yao, D. Johnson, P. J. Evans, and P. J. Evans // Orthobullets. – 2021. https://www.orthobullets.com/hand/6034/scaphoid-fracture
24. *Nickel-titanium* arched shape-memory alloy connector combined with bone grafting in the treatment of scaphoid nonunion / P. Y. Zhou, L. Q. Jiang, D. M. Xia, J. H. Wu, Y.Ye, and S. G. Xu // European J. of Medical Res. – 2019. – **24**, № 1. – 27 p.
25. *3D computational* anatomy of the scaphoid and its waist for use in fracture treatment / M. D. Ahrend, T. Teunis, H. Noser, F. Schmidutz, G. Richards, B. Gueorguiev, and L. Kamer // J. of Orthopaedic Surgery and Res. – 2021. – **16**, № 1.
26. *Ashman R. B. and Rho J. Y.* Elastic modulus of trabecular bone material // J. Biomech. – 1988. – **21**, № 3. – P. 177–181.
27. *Mehrabi R., Dorri M., and Elahinia M.* Finite element simulation of NiTi umbrella-shaped implant used on femoral head under different loadings // Bioengineering. – 2017. – **42**, № 4. – 23 p.
28. *Marsell R., and Einhorn T. A.* The biology of fracture healing // Injury. – 2011. – **42**, № 6. – P. 551–555.
29. *In vivo* cyclic axial compression affects bone healing in the mouse tibia / M. J. Gardner, M. C. van der Meulen, D. Demetrakopoulos, T. M. Wright, E. R. Myers, and M. P. Bostrom // J. of Orthopaedic Res.: Official Publication of the Orthopaedic Res. Soc. – 2006. – **24**, № 8. – P. 1679–1686.
30. *Nomura S. and Takano-Yamamoto T.* Molecular events caused by mechanical stress in bone // Matrix Biology. – 2000. – **19**, № 2. – P. 91–96.
31. *Laros G.* Fracture Healing: Compression vs Fixation // Archives of Surgery. – 1974. – **108**, № 5. – P. 698–702.
32. *Biomechanical* evaluation of shape-memory alloy staples for internal fixation–an in vitro study / Q. J. Hoon, M. H. Pelletier, C. Christou, K. A. Johnson, and W. R. Walsh // J. Exp. Ortop. – 2016. – **3**. – 19 p.

Received 05.10.2021